Neodymium and hafnium boundary contributions to seawater along the West Antarctic continental margin

Jörg Rickli[a,b*], Marcus Gutjahr[c], Derek Vance[a], Mario Fischer-Gödde[d], Claus-Dieter Hillenbrand[e], Gerhard Kuhn[f]

[a] ETH Zurich, Institute of Geochemistry and Petrology, ETH Zurich, Clausiusstrasse 25, 8092 Zurich, Switzerland

[b] Bristol Isotope Group, School of Earth Sciences, University of Bristol, Wills Memorial Building, Bristol BS8 1RJ, UK

[c] GEOMAR Helmholtz Centre for Ocean Research Kiel, Wischhofstraße 1-3, 24148 Kiel, Germany

[d] Institut für Planetologie, Westfälische Wilhelms-Universität Münster, Wilhelm-Klemm-Strasse 10, 48149 Münster, Germany

[e] British Antarctic Survey, High Cross, Madingley Road, Cambridge CB3 0ET, UK

[f] Alfred Wegener Institute, Columbusstrasse, 27568 Bremerhaven, Germany

* Corresponding author. Tel.: +41 44 632 35 62, E-mail address: joerg.rickli@erdw.ethz.ch (J. Rickli)

Further email addresses:

Marcus Gutjahr: mgutjahr@geomar.de

Derek Vance: derek.vance@erdw.ethz.ch

Mario Fischer-Gödde: m.fischer-goedde@uni-muenster.de

Claus-Dieter Hillenbrand: hilc@bas.ac.uk

Gerhard Kuhn: Gerhard.Kuhn@awi.de

Word count: 6537 in the main text

Abstract

Neodymium and hafnium isotopes and elemental concentrations (Sm, Nd, Hf, Zr) have been measured in three water column profiles south of the Antarctic Circumpolar Current in, and to the east of the Ross Sea, in conjunction with five bottom water samples from the Amundsen Sea Embayment.

Neodymium and hafnium both appear to be released from sediments in the Embayment. In the case of Nd, this is reflected in radiogenic isotope compositions (ε_{Nd} up to -5.4) and highly elevated concentrations (up to 41 pmol/kg). Hafnium isotopes, on the other hand, are only very slightly altered relative to the open ocean sites, and boundary release is most prominently indicated by elevated concentrations (> 1 pmol/kg versus ~0.7 pmol/kg). There is also a local input of both Hf and Nd at the Marie Byrd Seamounts, which leads to Nd isotope compositions as radiogenic as -3.1, and hafnium shifted to less radiogenic compositions in local bottom water.

A compilation of the new data with literature data reveals a consistent view of the influence of Antarctica on the Nd isotope composition in Lower Circumpolar Deep Water (LCDW) and Antarctic Bottom Water (AABW). Sector specific Nd addition shifts AABW formed in the Atlantic sector to less radiogenic isotope compositions (average ε_{Nd} = -9) relative to LCDW (average ε_{Nd} = -8.4), whereas AABW in the Pacific sector is shifted to more radiogenic values (average ε_{Nd} = -7).

The evolution towards more radiogenic ε_{Nd} with depth in LCDW in the Pacific sector is likely to reflect admixture of AABW but, in addition, is also controlled by boundary exchange with the slope as observed at the Marie Byrd Seamounts.

Hafnium isotopes are relatively homogenous in the data set, ranging between ε_{Hf} = +2 and +3.8 for most samples, excluding less radiogenic compositions in deep waters close to the Marie Byrd Seamounts. The Hf isotope composition in the Pacific sector is, however, slightly less radiogenic than in the Atlantic, corresponding to an average of +3 relative to an average of +3.8. This probably reflects unradiogenic Hf inputs from Antarctica to the Pacific sector, which are vertically homogenized by reversible scavenging. The Hf isotope heterogeneity in LCDW between both sectors is likely to indicate a shorter seawater residence time for Hf than for Nd, which is consistent with the dissolved – particulate phase partitioning of both elements.

Keywords: neodymium; hafnium; seawater; Southern Ocean; radiogenic isotopes

1. Introduction

The reconstruction of past ocean circulation using seawater-derived neodymium (Nd) isotope compositions has a longstanding tradition on Quaternary and longer timescales (see reviews in Frank, 2002 and Goldstein and Hemming 2003). The application often relies on the assumption of "quasi-conservative" behaviour of Nd isotopes as a water mass tracer, which assumes that the seawater Nd isotope composition at a given location primarily reflects the relative contribution of Nd from the mixing of water masses rather than non-

advective processes such as scavenging and vertical regeneration in the water column or fluxes from sediment (Goldstein and Hemming, 2003; Siddall et al., 2008). A variety of studies have, however, shown that Nd can be released or exchanged along continental margins from shallow to abyssal settings (Carter et al., 2012; Lacan and Jeandel, 2001; 2005a,b, Rickli et al., 2009; Wilson et al., 2012), implying non-conservative behaviour at least close to the seabed. In addition, inherited continental FeMn oxyhydroxides and sediment redistribution processes, for example along ridges, can also obscure authigenic seawater records (Bayon et al., 2004; Gutjahr et al., 2008). Some locations, such as parts of the Atlantic sector of the Southern Ocean, appear to be unaffected by these processes and yield robust information on the temporal variability of North Atlantic Deep Water formation between glacials and interglacials (Piotrowski et al., 2005; Rutberg et al., 2000). In summary, it should be considered as observationally established that studies using Nd isotopes need to evaluate, on a site-by-site basis, to which degree temporal variations in sediment-derived ε_{Nd} can be ascribed to changes in ocean circulation.

Hafnium isotope variations in seawater have only been explored recently (Godfrey et al., 2009; Rickli et al., 2010, 2009; Stichel et al., 2012a,b; Zimmermann et al., 2009a,b) due to the low concentration of Hf in seawater and resulting analytical difficulties. The interest in Hf isotopes as a paleoceanographic tool is twofold. Early observations of Hf isotopes in FeMn crust and nodules, which record ambient seawater isotopic compositions (Zimmermann et al., 2009b), have suggested that Hf isotopes are positively correlated with Nd isotopes on a global scale (Albarède et al., 1998; David et al., 2001). Hafnium isotopes have thus been used to complement Nd isotopes as a

water mass tracer in the past (Chen et al., 2012; van de Flierdt et al., 2004). Furthermore, time series of Hf isotopes in FeMn crust have led to the suggestion that the congruency in Hf isotope weathering could vary with the intensity of physical weathering on the continents (Piotrowski et al., 2000; van de Flierdt et al., 2002). Therefore, the Hf isotopic evolution of seawater may carry information on variations in physical weathering intensity in the past. A few initial studies on Hf isotopes in rivers, however, suggest that the presence (or absence) of phosphates, as well as the hydrological conditions, may actually be more important for the congruency in Hf weathering than physical grinding of rocks by glacial activity (Bayon et al., 2006; Rickli et al., 2013). In general, the sources of seawater Hf are poorly constrained to date (e.g., Vervoort et al., 2011). For instance, it is not well documented whether Hf is released or exchanged along continental margins, as observed for Nd.

Whether and to which degree Nd or Hf behave conservatively in seawater can be tested through measurement of elemental and/or isotopic exchange fluxes along ocean margins. Such fluxes, if present, can affect Nd and Hf isotope records of past ocean circulation (a point previously made in Carter et al., 2012), as these records are obtained from sedimentary phases, which record Nd and Hf in ambient bottom water (e.g., Piotrowski et al., 2005; Zimmermann et al., 2009b). There is a need for a better understanding of such boundary processes to characterize their effect on the distribution of Nd and Hf isotopes on a larger scale, and to help quantify their contribution to the seawater elemental budgets of Hf and Nd. Modelling studies of the oceanic distribution of Nd isotopes indicate that the seawater budget may actually be dominated by boundary related processes, which could account for up to 90% of seawater Nd (Rempfer

et al., 2011; see also also Arsouze et al., 2007). For simplicity, we will refer to this interface generally as the ocean boundary, independently of the nature of the seafloor (soft sediments, hard ground) or the oceanographic setting (open ocean, continental shelf).

The release of Nd at a boundary can be compensated by a capture of similar magnitude by scavenging (e.g., Lacan and Jeandel, 2005b). Hence the generic term "boundary exchange" has been introduced (Lacan and Jeandel, 2005a). Little is known about the importance of this process so far with respect to Hf. Observed Hf and zirconium (Zr) concentration profiles across the Celtic Sea shelf in the northeastern Atlantic Ocean indicated no boundary source for both elements (Godfrey et al., 1996). Boundary release of Hf was, however, suggested to happen in the Bay of Biscay based on one single anomalous observation of Hf isotopes and concentrations at 2000 m depth (Rickli et al., 2009). Release of Hf to the surface ocean from basaltic ocean islands seems to be common (Rickli et al., 2010; Stichel et al., 2012b). Boundary fluxes may also explain deep-water maxima in Zr concentrations observed in the open Pacific Ocean (McKelvey and Orians, 1998, 1993). In addition, mixing considerations using Hf isotopes have been used to argue for the release of Hf from the shelf of the Canadian Basin in the Arctic Ocean (Zimmermann et al., 2009a). The mixing end-member compositions of Pacific inflow and riverine inputs were, however, relatively poorly constrained.

The aim of the present study is to constrain processes of Nd and Hf release and exchange at the seawater/seafloor interface off and on the West Antarctic continental margin, using radiogenic isotope and concentration data. This study area is particularly suitable since continent-derived glacial sediments deposited

along the margin likely experienced very little chemical alteration preceding deposition, therefore representing reactive immature sediments (e.g., Anderson, 2007; Hillenbrand et al., 2013; Wadham et al., 2010). Hence, compared with other near-continental marine settings, elemental and isotopic exchange may be particularly pronounced offshore West Antarctica.

2. Regional setting and hydrography

2.1 Hydrography

The circulation of the Southern Ocean is dominated by the eastward flowing Antarctic Circumpolar Current (ACC), which is bounded to the north by the Subtropical Front (STF) and to the south by its southern boundary (SBACC, Fig. 1, Orsi et al., 1995). The ACC essentially extends from the surface to abyssal depths and eastward transport is mainly concentrated in the Subantarctic and the Polar Front (SAF, PF, Talley et al., 2011 and references therein). Beneath Antarctic Surface Water (AASW), the ACC is divided into Upper Circumpolar Deep Water (UCDW), Lower Circumpolar Deep Water (LCDW) and Antartic Bottom Water (AABW). Upwelling of LCDW south of the SBAAC and modification by sea ice formation processes on the shelf of the Weddell Sea, the Ross Sea and Adélie coast and further less significant shelf areas leads to the formation of AABW (Orsi et al., 1999). In contrast to LCDW, AABW is not a circumpolar water mass. There is no free exchange of bottom waters between the Atlantic, Pacific and Indian sectors, due to several sills between the basins (Orsi et al., 1999). As a result the regional bottom waters, including Weddell Sea, Adélie and Ross Sea Bottom waters, are characterized by specific salinity-temperature properties (Orsi and Whitworth, 2005; Orsi et al., 1999).

The area of the study is situated south of the SBACC, within and east of the Ross Sea Gyre (Fig. 1). Three major water masses can be distinguished, namely AASW, LCDW and AABW (Fig. 2). The water mass transitions as used here follow Whithworth et al. (1998) and are based on neutral densities γ^n. The boundary between AASW and underlying LCDW corresponds to a neutral density isopycnal of 28.00 kg/m^3, which is in a depth range between 100 and 250 m (Talley et al., 2011). The vast majority of the water column beneath AASW is occupied by LCDW ($28.00 < \gamma^n < 28.27$) or modifications of it on the shelf (Arneborg et al., 2012; Orsi et al., 1995; Whitworth et al., 1998). Throughout the deep Pacific basin LCDW is underlain by Antarctic Bottom Water (AABW, $\gamma^n > 28.27$), predominantly formed in the Ross Sea (Jacobs et al., 1970; Orsi and Wiederwohl, 2009). The transition between LCDW and AABW is as shallow as 2400 m to the north of the Ross Sea and deepens to more than 4000 m west of the tip of South - America (Orsi et al, 1999; their Fig. 6).

2.2 Regional Geology

The eastern Ross Sea and the Amundsen Sea are mainly bordered by Marie Byrd Land (Fig. 1), which is structurally sub-divided into two major provinces. The western and/or interior Ross Province consists of early- to mid-Palaeozoic magmatic and metasedimentary sequences. The eastern or Amundsen Province has no exposed Palaeozoic metasediments and outcropping magmatic successions result from early Palaeozoic to late Mesozoic calc-alkaline plutonism and Cenozoic volcanism (Kipf et al., 2012; LeMasurier and Rex, 1991; Mukasa and Dalziel, 2000; Pankhurst et al., 1998). The underlying lithosphere of the two provinces can be distinguished based on Nd isotope data, where Ross province

successions have slightly older model ages (1300-1500 Ma) than those of the Amundsen province (1000-1300 Ma, Pankhurst et al., 1998).

Knowledge about the origin of the Marie Byrd Seamounts (MBS, Fig. 1) is to date largely based on one petrographic study (Kipf et al., in press). This group of intraplate volcanic seamounts is located offshore the Amundsen Sea Embayment (ASE). Most of the seamounts formed between 65 Ma and 56 Ma, hence well after the full development of the Pacific-Antarctic ridge and separation of New Zealand from West Antarctica. Petrographically, rocks of the MBS can be classified as (ultra-)mafic sequences of the alkaline differentiation series. Pliocene and Pleistocene magmatic ages for two of the seamounts suggest that the origin of the MBS is not simply related to a single hot spot (Kipf et al., in press).

3. Sampling and methods

Seawater was collected in 10 l Niskin bottles attached to a CTD rosette during the scientific cruise of R/V Polarstern ANT-XXVI/3 between February and April 2010 in the Pacific sector of the Southern Ocean (Fig. 1, Table 1). A first depth profile was sampled in the Ross Sea (St 116), one on the continental rise in the Amundsen Sea (St 143) and a third at the MBS, more specifically at the Haxby Seamount (St 253). Stations 116 and 143 lie south of the SBACC in the Ross Sea Gyre, while station 253 is approximately on the SBACC. Five stations that sampled bottom water within 1 to 2 m of the seafloor on the continental shelf in the ASE were also included. Based on the hydrography outlined in section 2.1 AABW was sampled below 3200 m at St 116, and at Station 143 on the continental rise (Fig. 2, Table 1). The deep water bathing the Haxby Seamount,

on the other hand, is LCDW. All shelf bottom water stations sampled in the ASE retrieved LCDW. The two stations closest to the ice shelf front (St 155, 176) sampled deep waters with lower salinities and slightly lower densities than the shelf stations further offshore. These waters hence represent Modified Circumpolar Deep Water (MCDW, Whitworth et al., 1998). The fact that samples were taken only south of the SBACC, where UCDW is not observed (Orsi et al., 1995), means that a distinction between LCDW and UCDW is not necessarily relevant to this study. For clarity and when comparing the new data to literature data we, however, adhere to the specific abbreviation of Lower Circumpolar Deep Water.

Hafnium and neodymium for isotope measurements were enriched from 10 to 16 litres of unfiltered seawater on board the ship using Fe-co-precipitation (see for instance Rickli et al., 2009). Concentration aliquots for isotope dilution (Zr, Hf, Sm and Nd) were collected separately in acid-cleaned 250 ml bottles and acidified to pH <2. Isotope and concentration samples were further processed at the clean lab facilities at the University of Bristol.

A detailed description of the chemical and mass spectrometric procedures is given in the appendix. As detailed therein, estimated external reproducibility for Hf and Nd isotopes corresponds to 0.9 and 0.15 epsilon units, respectively (2 SD). Neodymium isotopes and elemental concentrations were measured on a ThermoFinnigan Neptune MC-ICPMS at the University of Bristol, UK. Hafnium isotopes were measured on a ThermoFinnigan Neptune Plus instrument at the University of Munster, Germany. Due to low Hf concentrations in shallow water samples, high blank to sample ratios (> 5%), as well as large internal uncertainties on the isotope analyses (1-2 ε_{Hf}, 2 SEM), precise data are not

available. Hence these data points are not reported. Elemental concentrations are reproducible within 1% for Zr, Sm, Nd and within 5% for Hf (1 SD).

4. Results

4.1 Concentrations of Zr, Hf and Nd

Hafnium and zirconium show very similar depth profiles at the continental rise, the Haxby Seamount and in the Ross Sea (Tab. 1, Fig. 3a,b). Both elements are depleted in low salinity surface waters, yielding concentrations below 0.5 and 100 pmol/kg, respectively. Below 200 m water depth the concentrations increase relatively monotonically to ~0.9 and ~280 pmol/kg in the open water column. More elevated concentrations are, however, observed close to the seafloor, in particular at the continental rise where a maximum concentration of 1.12 pmol/kg Hf and 348 pmol/kg Zr is reached 5 m above the seafloor. The observations on the shelf are different for Hf and Zr. Hafnium concentrations are much higher on the shelf (> 1 pmol/kg) than observed for the open ocean at the corresponding depth (~0.7 pmol/kg), while the Zr concentrations are only slightly elevated (~250 relative to ~220 pmol/kg). The continental rise, and to a lesser degree the Haxby Seamount, stations do show some Hf enrichment in this depth interval. This is evident between 600 and 1500 m at the continental rise station (Hf > 0.75 pmol/kg) and in 500 m water depth at the Haxby Seamount (Hf = 0.8 pmol/kg).

Some of the above features become more evident when Zr/Hf ratios are examined (Fig. 3d). The shelf waters and the continental rise waters at 500 – 1500 m are characterized by distinctly low Zr/Hf ratios (below 300). Apart from that Zr/Hf ratios are fairly uniform. Each depth profile, however, shows elevated

Zr/Hf ratios in low salinity surface waters (Zr/Hf > 375) and slightly lowered Zr/Hf ratios close to the seafloor (Zr/Hf <320).

Although the distribution of Nd (and Sm) is generally similar to that of Hf, there are a few notable differences (Fig. 3c). In contrast to Hf and Zr, Nd is not distinctly depleted in surface waters at St 143 and 253 and even shows a slight surface enrichment in the Ross Sea. In addition, there is no enrichment of Nd at the continental rise around the depth of the shelf stations, yet a slight enrichment is observed in the Ross Sea.

Hafnium/neodymium ratios are elevated and exceed 0.03 on the shelf, and at the corresponding depth interval at the continental rise station, implying a stronger enrichment for Hf than for Nd in shelf waters (Fig. 3e). Elevated Hf/Nd is also observed at 500 m at the Haxby Seamount, resulting from the aforementioned high Hf concentration at this depth. The described concentration patterns for Hf and Nd result in low Hf/Nd ratios in low salinity surface waters (Hf/Nd <0.02). Apart from these two prominent features in Hf/Nd ratios - the high ratios associated with the shelf and the low ratios in the surface ocean - Hf/Nd ratios are quite uniform, predominantly between 0.02 and 0.03. Seawater close to the seafloor at the deep-sea stations (St 116, 143, 253) has slightly higher Hf/Nd ratios than the neighbouring samples above. This is, however, not a very pronounced phenomenon.

4.2 Seawater Hf and Nd isotope compositions

The reported seawater Hf isotope compositions are overall very homogeneous (Fig. 3f). Apart from the two deepest samples at the Haxby Seamount and the shallowest sample on the continental rise, the seawater Hf isotope composition

ranges between ε_{Hf} = +2 and +3.8. Under the conservative assumption of a representative external reproducibility of ± 0.9 ε_{Hf} (2 SD, see appendix for details), these values are barely distinguishable. However, the shelf waters are consistently among the least radiogenic observed in their depth interval, which may be a real but minor effect associated with shelf processes (as discussed in section 5.4, 5.5).

The observed variation in seawater Nd isotope compositions is very large, ranging between ε_{Nd} = -9.1 and -3.1. The deep-sea stations stations show virtually identical Nd isotope profiles between 500 and 3000 m, whereby the Nd isotope composition gradually increases from ε_{Nd} = -9 to -7.8 (Fig. 3g). Above 300 m water depth in AASW the Nd isotope compositions shows some variation, with the surface waters at the continental rise (ε_{Nd} = -8.1) being more radiogenic than at the Haxby Seamount (-8.5) and in the Ross Sea (-8.8). Below 3000 m Nd isotopes display variable trajectories to more radiogenic compositions. The most extreme occurs at the Haxby Seamount, where an ε_{Nd} of -3.1 is reached close to the seafloor, opposing the trend to less radiogenic Hf isotopes observed at this site (Fig. 3f). Bottom waters on the ASE shelf are consistently more radiogenic (between ε_{Nd} = -7.4 and -5.4), relative to the constant value of -8.8 observed at the neighbouring open ocean sites.

5. Discussion

5.1 Neodymium concentrations in the Southern Ocean

From an oceanographic point of view it is more appropriate to use neutral density rather than water depth when assessing processes that control elemental

concentrations and isotopes other than circulation. Similar neutral densities for LCDW and AABW imply similar water mass properties (salinity, temperature, Fig. 2) and hence provide a good means of comparing concentrations and isotopes within a water mass at different locations in the Southern Ocean. Comparison based on depth is less meaningful, as the transition between LCDW and AABW, for instance, is regionally highly variable (see section 2.1). Hence, we will discuss our isotope and concentration data mainly in relation to neutral density.

There have been two comprehensive studies, which report on Nd isotope composition and concentration of water masses in the Southern Ocean. Stichel et al. (2012a) studied the Atlantic sector of the Southern Ocean including the Weddell Sea Gyre, while Carter et al. (2012) investigated the eastern Pacific sector including sites in the ASE (Fig. 1, 2). The new data are consistent with the earlier observations in the ASE, whereby Nd concentrations are strongly elevated (up to 40 pmol/kg) relative to the neighbouring open ocean sites (typically 15 to 25 pmol/kg, Fig. 4). This indicates Nd release from shelf sediments, which is also supported by the Nd isotope data (section 5.2). The lack of filtration in the present study could, in principle, cause elevated Nd concentrations due to particle leaching. The expected effect on Nd concentrations from leaching should probably not exceed 5% of the dissolved concentration (Jeandel et al., 1995). Neodymium concentrations and isotope data for the ASE are, however, consistent with the results on the filtered samples of Carter et al. (2012), suggesting that particle leaching does not affect the Nd budget significantly (Fig. 4c,d). Although many of the new observations in the open water column are in agreement with the observed relationship between

neutral density and Nd concentrations from the eastern Pacific sector (Fig. 4c), four elevated concentrations are observed between $\gamma^n \sim 28.1$ and 28.2. These observations are in the density range of Nd - enriched shelf waters, which also hints at the shelf as the source of Nd.

The Nd concentrations that are apparently not affected by shelf processes in the open Southern Ocean show a linear increase with neutral density (Fig. 4c). Such a linear evolution is consistent with a strong influence of reversible scavenging on the distribution of Nd (Bacon and Aderson, 1982; Little et al., 2013; Siddall et al., 2008), and also in agreement with the interpretation that opal dissolution releases Nd with depth (Stichel et al., 2012a). The increase in Nd with neutral density in the Pacific sector is somewhat stronger than in the Atlantic (Fig. 4c), which may imply more efficient dissolution of settling particles. However, an exclusive control of the Nd concentrations by reversible scavenging can be precluded, as there is a Nd isotope trend with neutral density (Fig. 4d), which implies addition of isotopically different Nd by advection and/or at the local boundary. These possibilities are further evaluated in the following section.

5.2 Neodymium isotopes in the Southern Ocean

Antarctic Surface Water offshore the West Antarctic margin shows slightly more radiogenic Nd isotope compositions than the core of LCDW beneath it (Fig. 4a). The observed Nd isotope compositions on the coast, ranging between -6.3 and -1.3 (Pankhurst et al., 1998), indicate that this is likely to reflect radiogenic Nd contributions from Antarctica to AASW. In support of this interpretation, the feature is most pronounced at the continental rise station, which is closest to the Antarctic ice shelf margin (Fig. 1).

The S-θ properties of LCDW in the ACC show some variation around Antarctica (e.g., Orsi et al., 1999). This reflects the inheritance of a salinity maximum from NADW in the Argentine Basin, which is progressively eroded by addition of fresher water to the ACC from the Indian and Pacific Ocean. Given the distinctive ε_{Nd} of NADW, some variation in the Nd isotope composition of LCDW could be expected if the full range in salinity and potential temperature of LCDW were covered in the available data sets. This is, however, not the case (compare Fig. 2b and Fig. 5 of Orsi et al., 1999) and the available Nd isotope data on LCDW is, indeed, relatively homogenous. If the deepest samples at the Haxby Seamount (discussed in 5.5) and the waters from the ASE are excluded, an average Nd isotope composition of all remaining data, including the data of Carter et al. (2012) and Stichel et al. (2012a), corresponds to -8.4 ± 0.8 (2 SD). There is, however, a systematic increase in ε_{Nd} with neutral density in LCDW in the Pacific sector (Fig. 4d), which will be discussed below.

Compared with the open ocean situation described above, the Nd isotope composition of LCDW (and MCDW) is strongly influenced by local inputs in the ASE. Carter et al. (2012) and the present study document the release of radiogenic Nd to the water column in this area of the shelf, which results in Nd isotope compositions as radiogenic as -4.5 (Fig. 4d). These observations are consistent with the Nd isotope composition of sediments from the ASE ranging between -2.7 and -0.8 (Carter et al., 2012). The composition of the sediments in the ASE is in turn consistent with the observed Nd isotope compositions in rocks west of the ASE, which are relatively variable but which range between -6.7 and +4 (Pankhurst et al., 1998).

Outside the ASE the Nd isotope compositions are very similar for a given neutral density along most parts of the West Antarctic margin, showing a gradual increase of ε_{Nd} with γ^n (this study; Carter et al., 2012, Fig. 4d). The variability in Nd isotope compositions with γ^n is likely to reflect variable inputs from Antarctica, which could occur through different processes. Freshly forming AABW in the Ross Sea is probably affected by Nd release as observed in the ASE and will possibly also exchange, or simply gain, Nd as it sinks along the continental slope and mixes with LCDW (e.g., Orsi et al., 1999). In addition, it is plausible that the local seafloor releases radiogenic Nd, which is certainly the case at the Haxby Seamount (Fig. 3g, section 5.5).

The relative weighting of radiogenic Nd contributions to LCDW by direct boundary exchange with the continental slope, versus advected Nd within AABW, is not clear at present. A direct control by boundary exchange would imply that the impact of Antarctica should fade with increasing distance from the continent, while an alteration of the Nd isotope composition of AABW during its formation would mean that the radiogenic Nd signal should also be observable away from Antarctica, something that remains to be documented in more detail. Carter et al. (2012) reported a water column that is relatively clearly structured in ε_{Nd} north of the Polar Front (their site 022), arguing for advection of Nd within AABW. Tazoe et al. (2007) on the other hand reported virtually constant ε_{Nd} (-8.9 ± 0.2) in the Ross Sea gyre (see Fig. 1 for the location).

In contrast to LCDW, AABW shows clear differences between the Pacific and the Atlantic sector of the Southern Ocean in terms of its Nd isotope composition. While AABW is less radiogenic than LCDW in the Atlantic (average ε_{Nd} = -9.0), it

is more radiogenic than LCDW in the Pacific sector (average ε_{Nd} = -7.0, Fig. 4d). The different processes in the areas of deep-water formation, which are mostly the Ross Sea in the Pacific and the Weddell Sea in the Atlantic sector, lead to characteristic S-θ properties for the respective bottom waters (e.g., Orsi et al., 1999). Ross Sea Bottom Water, for instance, is relatively salty, as a large fraction of the water is produced by brine rejection in polynias on the Ross Sea shelf (e.g., Budillon et al., 2011; Orsi and Wiederwohl, 2009). The basin specific S-θ properties are largely preserved, as several sills prevent free exchange of AABW between the Atlantic, Pacific and Indian sectors (e.g., Orsi et al, 1999). The primary cause of the variable Nd isotope compositions of AABW between the Pacific and the Atlantic is thus likely to be differing Nd isotope compositions of rocks and sediments in the respective areas of deep-water formation. Potential source rocks for unradiogenic Nd in the Atlantic sector have been identified (Stichel et al., 2012a). For the Pacific sector the observed shift in the Nd isotope composition of AABW relative to LCDW is broadly consistent with the observed Nd composition along the coast (Pankhurst et al., 1998). These compositions tend to become less radiogenic westwards, from an average ε_{Nd} of -1.3 to the west of the ASE, to -4.6 in the hinterland of the western Amundsen Sea, and to -6.3 in the hinterland of the easternmost Ross Sea. As noted above, Nd addition during sinking of AABW to the deep sea and local Nd addition as observed at the Haxby Seamount (to LCDW) is likely to occur as well.

5.3 Hafnium concentrations in the Southern Ocean

In contrast to the relatively small fraction of Nd associated with particles in seawater (usually <5%, Jeandel et al., 1995), a significant fraction of Hf can be

particle-associated. A study from the north Pacific reported variable particle-associated Hf fractions, corresponding to 2% of the dissolved Hf in intermediate waters and up to 25% in shallow and deep waters (Firdaus et al., 2008). However, the Zr/Hf ratios of the unfiltered water samples (319 ± 76, for 30 samples of Pacific Deep Water) were very similar to the filtered ones (341 ± 34), yet very different to crustal ratios of 71 (e.g., Rudnick and Gao, 2003). This suggests that, at least in the north Pacific, particulate Hf and Zr is predominantly seawater derived.

As for Nd, the increase in Hf concentration with neutral density is linear in the Atlantic sector of the Southern Ocean (Fig. 5c), and also strongly correlated with silicon concentrations (Stichel et al, 2012a). Most of the samples in the Pacific sector are shifted to higher concentrations for a given neutral density when compared to data from the Atlantic sector (Fig. 5c,d). Based on the observations of particle-associated Hf from the North Pacific, enrichment by 25% could easily reflect a contribution from leached particles. Bottom nepheloid layers were previously reported from the shelf and continental rise of the western Ross Sea (Budillon et al., 2006; Capello et al., 2009) to the west of station 116 (Fig. 1), implying that a leached fraction from particulates could be much larger than 25% for some of the samples reported in this study. Upon visual inspection, water samples taken as close as 1-2 m above the seafloor were, however, completely clear, indicating little disturbance of the seafloor during the cruise. Hence, an enrichment of the deepest samples at the open ocean sites by a factor of up to 1.8 and on the shelf by a factor of up to 3 compared to the Atlantic data (Fig. 5c,d) is unlikely to result solely from leaching. Instead, these elevated Hf concentrations probably also reflect dissolved Hf fluxes, which is in agreement

with the observations made for Nd concentrations and isotopes (this study; Carter et al., 2012). Transmissivity data, which could confirm the presence or absence of nepheloid layers during sampling, are unfortunately not available.

Zirconium/Hafnium ratios could, in principle, provide a monitor of leached crustal Zr and Hf contributions. Recent observations suggest that Zr is progressively enriched over Hf in seawater with increasing deep-water mass age, resulting in molar ratios up to 500 in the North Pacific (Fig. 6, Firdaus et al., 2011). In settings close to the coast or near the surface ocean, filtered seawater Zr/Hf ratios as low as crustal ratios were reported (Godfrey et al., 1996; McKelvey, 1994), implying that the relatively low Zr/Hf ratios between 180 and 270 observed in the ASE do not necessarily reflect large contributions from the leaching of particulates but are consistent with a seawater origin (Fig. 6).

5.4 Hafnium isotopes in the Southern Ocean

Within the reported analytical uncertainty (± 0.9 ε_{Hf}, 2SD), Hf isotopes are very uniform in most waters analysed in this study (Fig. 5b,e). A clear shift to unradiogenic Hf isotope compositions is, however, observed in the two deepest samples at the Haxby Seamount, which points to an external source as further discussed in section 5.5. Excluding these two observations AABW and LCDW are virtually identical in their Hf isotope compositions, with an average ε_{Hf} of +2.9 (± 1, 2SD) and +3.1 (± 1.2, 2SD), respectively (Fig. 5e, p-value for two sided Wilcoxon rank sum test = 0.37). Similarly, no significant differences are observed between AABW and LCDW in the Atlantic sector ($\varepsilon_{Hf\text{-}AABW}$ = +4.1 ± 1, $\varepsilon_{Hf\text{-}LCDW}$ = +3.7 ± 1.3, p-value = 0.19, Stichel et al., 2012a). There is thus no evidence for

differences in the Hf isotope compositions of LCDW and AABW in either studied areas based on our current ability to measure seawater Hf isotope compositions.

Deep waters in general, including AABW and LCDW, are, however, slightly more radiogenic in the Atlantic sector than in the Pacific sector ($\varepsilon_{Hf\text{-}Atl}$ = +3.8 ± 1.2, $\varepsilon_{Hf\text{-}Pac}$ = +3 ± 1.1, p-value <0.001). In principle, there are two reasons that could explain the difference. On one hand, it could be that the lack of filtration produces the offset. Fine terrigenous clay sized particles, for instance, could be less radiogenic than ambient seawater, and leaching of these particles may cause the offset. Such a scenario cannot be fully precluded, which means that filtration is crucial for Hf isotopes, especially when studying boundary processes. Generally, it is not clear what effect leaching of clays would have, as the released Hf could even shift seawater values to more radiogenic compositions (Chen et al., 2013a). The second explanation is that spatial variations in dissolved Hf isotopes are real and reflect isotopically variable Hf inputs from Antarctica, which are not homogenized laterally but redistributed throughout the water column by intense reversible scavenging. In this case, it would seem that the Atlantic sector of the Southern Ocean is unaffected by local inputs, as the Hf isotope composition does not change as the coast is approached (Stichel et al., 2012a). Hafnium isotope compositions close to the coast in the Atlantic sector are also in agreement with the long term deep water ε_{Hf} in this basin, as recorded in ferromanganese nodules ($\varepsilon_{Hf\text{-}Atl}$ = +3.9, van de Flierdt et al., 2006). Alternatively the released local Hf isotope signature in the Atlantic may be coincidentally very similar to compositions seen further offshore. Relatively unradiogenic Hf, however, seems to be released from Antarctica in the Pacific sector of the Southern Ocean. Although there is no strong evidence for such a release of unradiogenic Hf in the

ASE, the shelf samples do yield consistently low Hf isotope composition, within the observational range (Fig. 3f). A local reflection of Hf inputs implies a short residence time of Hf, which is consistent with observations in the Baltic Sea (Chen et al., 2013b). Further support for a short residence time of Hf relative to Nd may actually lie in the dissolved - particulate partitioning of both elements. A larger particle-associated fraction of Hf is likely to reflect faster absorption and a correspondingly lower seawater residence time (e.g., Rempfer et al., 2011).

5.5 Processes promoting Hf and Nd boundary exchange / release

The Nd and Hf isotope compositions observed in the deepest samples at the Haxby Seamount are extreme when compared with the other results obtained in this study (Fig. 3f,g). Neodymium is well known to exchange isotopically with surrounding lithologies along ocean margins, especially when these margins are basaltic (Lacan and Jeandel, 2001; 2005; Wilson et al., 2012; Pearce et al. 2013). The average ε_{Nd} of rock samples from the MBS corresponds to +4.4 ± 1.8 (2 SD, n=15, Kipf et al., in press). This, and the data for bottom water at St 253, would be consistent with the addition of basaltic Nd to bottom water at this site. Since the Nd concentrations are similar to the other observations at St 116 and 143 (Fig. 3c) Nd would need to be exchanged at the Seamount rather than simply added to the deep waters (e.g., Lacan and Jeandel, 2005).

However, the systematic and strong shift towards unradiogenic Hf in the bottom two samples at St 253, a shift that appears to be closely coupled to the shift towards radiogenic Nd, (Fig. 3f,g) is not consistent with the above explanation for the Nd isotopic shift. Rock data from the MBS yield an average ε_{Hf} of +4.1 ± 3.8 (2 SD, n=10, Kipf et al., in press). Addition of such material cannot

achieve the shift in Hf isotopes in bottom water at St 253, away from ε_{Hf} around +3 towards less radiogenic ε_{Hf} of -1 in the bottom-most sample. Any radiogenic Hf flux from the MBS, which was previously observed in surface ocean waters adjacent to mafic ocean islands (Rickli et al., 2010; Stichel et al., 2012b), is apparently not seen here.

An alternative possible interpretation of both the Nd and Hf data in bottom water at Station 253, and perhaps elsewhere, is illustrated in Fig. 7. In principle, both Nd and Hf of the appropriate isotopic composition could be supplied through relatively congruent remobilisation from sediments derived from the West Antarctic margin (van de Flierdt et al., 2002, 2007). In fact Fig. 7 indicates that bottom water coupled isotope compositions for the open ocean as well as for the ASE sites, are consistent with variable contributions from congruently released Hf and Nd from a single source with an isotopic composition close to the terrestrial array, given their gradual departure from the seawater towards the terrestrial array. The puzzle, however, is why such a signal is so clear at St 253 but is only just detectable in the ASE. The very radiogenic seawater Nd isotope compositions at St 253 may also imply combined contributions from MBS and Western Antarctica. An overwhelming dominance of sediment derived Nd from Western Antarctica in deep water at St 253 seems questionable, but is implied when comparing sediments from the ASE (ε_{Nd} = -2.7 to -0.8, Carter et al., 2012) with the most radiogenic seawater at the Seamount (ε_{Nd} = -3.1). Significant contributions to the seawater Hf budget from the Seamount are, however, precluded.

6. Conclusions

In contrast to the Atlantic sector of the Southern Ocean, the Pacific sector is characterized by a gradual change to more radiogenic Nd isotope compositions with water depth and neutral density. Observations in the Amundsen Sea Embayment indicate that the shelf is an important source of radiogenic Nd (this study; Carter et al., 2012), possibly due to the reductive dissolution of FeMn oxyhydroxides (e.g., Elderfield et al., 1987; Haley et al., 2004). Such release of Nd is likely to occur also in the Ross Sea, thereby affecting the Nd isotope composition of AABW during its formation. This conclusion is supported by Nd isotope compositions up to -6.3 in the densest (purest) measured AABW samples. In addition, boundary exchange of Nd outside the shelf area is observed at the Marie Byrd Seamounts, but may also occur at other sites. A combination of such boundary exchange processes on the slope and advection of radiogenic Nd within AABW is proposed to cause the gradual change of Nd isotope compositions with neutral density in LCDW and AABW, although their relative significance is not fully resolved at present. Sector specific Nd additions are clearly manifested in distinct Nd isotope compositions of the Antarctic Bottom Waters, corresponding to -7 in the Pacific sector of the Southern Ocean (this study, Carter et al., 2012) and to -9 in the Atlantic sector (Stichel et al., 2012a).

In contrast to the observed Nd isotopic variability, the seawater Hf isotope composition is remarkably constant between sampling sites along the West Antarctic continental margin, as well as with water depth. The reported analytical uncertainty on seawater Hf isotope measurements is, however, relatively large (± 0.9, 2 SD), implying that small variations may well exist.

Similar to water column data from locations within the Atlantic sector of the Southern Ocean (Stichel et al., 2012a), most Hf isotope compositions presented here show a narrow range, between ε_{Hf} = +2 to +3.8. The average Hf isotope compositions in the Pacific sector ($\varepsilon_{Hf\text{-}Pac}$ = +3 ± 1.1, 2 SD, combined observations on AABW, LCDW) are, however, slightly less radiogenic than in the Atlantic sector ($\varepsilon_{Hf\text{-}Atl}$ = +3.8 ± 1.2), which is likely to result from Antarctic inputs to the Pacific sector. The difference could, however, potentially also reflect the leaching of fine suspension in the present study, as the measurements were performed on unfiltered seawater samples.

While Nd derived from Antarctica has a clear impact at most sites studied here, any effect on Hf is less evident, especially in terms of causing seawater Hf isotopic variability. A relatively clear case can be made for boundary addition of Hf in the Amundsen Sea Embayment based on observed elevated Hf concentrations, accompanied by a subtle change towards lower ε_{Hf}. A much clearer shift towards unradiogenic Hf seawater compositions close to the Marie Byrd Seamounts (ε_{Hf} as low as -1) is also coupled to clearly more radiogenic Nd (ε_{Nd} as radiogenic as -3.1). The opposing trends in Hf and Nd isotopes at the Seamounts and in the Embayment are, in principle, consistent with the addition of congruently released Hf and Nd from Western Antarctica. At the Seamounts it may, however, also imply different dominating sources for each element. For Nd this source would be the radiogenic Seamounts themselves, meanwhile the Antarctic source rocks of unradiogenic Hf as well as the mechanism accounting for the source decoupling are not well constrained.

Acknowledgements

The crews and the shipboard scientific parties during RV *Polarstern* expedition ANT-XXVI/3 in 2010, especially chief scientist Karsten Gohl, are thanked for all their help during seawater sampling. Chris Coath and the Bristol Isotope Group are thanked for keeping the labs running smoothly. We thank the three anonymous reviewers and the editor Gideon Henderson for their comprehensive and valuable comments. This work was supported by Marie-Curie Fellowships to J.R. (Project No. 253117) and M.G. (Project No. 220941).

Figure and table captions

Table 1:

Sample locations, hydrographic details, elemental concentrations and Hf and Nd isotope compositions. Hafnium and neodymium isotope compositions are expressed in epsilon units as deviations from the CHondritic Uniform Reservoir (Bouvier et al., 2008; Jacobsen and Wasserburg, 1980. Also note that the cited literature Hf isotope data has been adjusted to the new value of Bouvier et al. for CHUR). External reproducibility corresponds to 0.9 ε_{Hf} and 0.15 ε_{Nd}, respectively (2 SD, see appendix for details). Water mass classification follows Whitworth et al. (1998).

Fig. 1:

Map showing the open ocean stations (blue) and the stations in the Amundsen Sea Embayment (red) from this study, as well as the sites of Carter et al. (2012, green), Stichel et al. (2012a, light grey) and Tazoe et al. (2007, black). Also shown are the southern boundary of the ACC (SBACC), the Polar, the Subantarctic and the Subtropical Fronts (Orsi et al., 1995). MBL: Marie Byrd Land, ASE: Amundsen Sea Embayment, MBS: Marie Byrd Seamounts. Map generated with GeoMapApp (http://www.geomapapp.org).

Fig. 2:

Salinity–temperature relationships for the water samples taken in this study and previous work on Hf and Nd isotopes in the Southern Ocean (Carter et al., 2012; Stichel et al., 2012a). (a) shows the CTD profiles for stations 116, 143 and 253 in conjunction with the properties of the sampled water. (b) shows data presented

in (a) at expanded scale focussing on the salinity range of LCDW and AABW. Illustrated literature data only include LCDW, AABW and waters from the ASE. Antarctic Bottom Waters are defined by neutral densities > 28.27 kg/m^3. MCDW refers to modified LCDW. (Neutral densities for the samples reported in Carter et al., 2012 were calculated from the original CTD data).

Fig. 3:

Seawater elemental concentrations (a-c), elemental ratios (d, e) and Hf and Nd isotope compositions (f, g) as a function of water depth. The shaded area in (f) indicates the average Hf isotope composition of the data set, excluding the two deepest samples at the Haxby Seamount, ± 2 SD (external reproducibility). Symbols are larger than the analytical uncertainty, except for Hf isotopes.

Fig. 4:

Neodymium concentrations and isotope composition in LCDW, AABW and the ASE (this study; Carter et al., 2012; Stichel et al., 2012a). (a, b) show the variations of Nd concentrations and isotope composition with depth, (c, d) with neutral density $\gamma^{\square}$. AASW samples from the present study are also shown in the depth profiles (bright blue circles). Note the smaller range in ε_{Nd} for (d) than for (b) allowing for a more detailed illustration of the difference in ε_{Nd} of AABW between the Atlantic and Pacific sector. The most radiogenic observations at the Haxby Seamount and in the ASE are only illustrated in (b). Symbols are larger than the analytical uncertainty.

Fig. 5:

Hafnium concentrations and isotope composition in LCDW, AABW and the ASE (this study; Stichel et al., 2012a). (a, b) show the variations of Hf concentrations and isotope composition with depth, (c, e) with neutral density γ^n. The solid line in (c) represents a linear regression line through the Hf concentration data from the Atlantic sector (Stichel et al., 2012a). The dashed line corresponds to enrichment by 25%, which can be expected, when comparing filtered to unfiltered samples (Firdaus et al., 2008; for details see section 5.3). (d) shows the enrichment factor of the samples from this study relative to the linear regression line in (c).

Fig. 6:

Compilation of seawater Zr/Hf ratios. All literature data was obtained on filtered seawater (David, 1994; Firdaus et al., 2011; Godfrey et al., 1996). Open red and green symbols represent sampling sites closest to the coast, which usually show seawater Zr/Hf similar to crustal ratios of 71. The unfiltered samples reported in the present study (symbols as in Fig. 4) are not anomalous in terms of their Zr/Hf ratios, providing no clear evidence for crustal contributions from the leaching of suspended particles.

Fig. 7:

Coupled Hf and Nd isotope compositions in deep waters from the Southern Ocean (Stichel et al., 2012a; this study). The terrestrial array represents the correlation of Hf and Nd isotopes in rocks (Vervoort et al., 2011), while the seawater array describes their relationship in seawater, as well as in FeMn crust and nodules (e.g., Albarède et al., 1998; Rickli et al., 2009). The deep waters from

the Pacific Sector, including the samples from the ASE, trend towards the terrestrial array arguing for congruently released inputs from Western Antarctica. Also indicated are the Nd isotope compositions of sediments in the ASE (green band, Carter et al., 2012).

References

Albarède, F., Simonetti, A., Vervoort, J.D., Blichert-Toft, J., Abouchami, W., 1998. A Hf-Nd isotopic correlation in ferromanganese nodules. Geophys. Res. Lett. 25, 3895-3898.

Anderson, S.P., 2007. Biogeochemistry of glacial landscape systems, Annual Review of Earth and Planetary Sciences. Annual Reviews, Palo Alto, pp. 375-399.

Arneborg, L., Wahlin, A.K., Bjork, G., Liljebladh, B., Orsi, A.H., 2012. Persistent inflow of warm water onto the central Amundsen shelf. Nature Geoscience 5, 876-880.

Arsouze, T., Dutay, J.C., Lacan, F., Jeandel, C., 2007. Modeling the neodymium isotopic composition with a global ocean circulation model. Chem. Geol. 239, 165-177.

Bacon, M.P., Anderson, R.F., 1982. Distribution of thorium isotopes between dissolved and particulate forms in the deep-sea. Journal of Geophysical Research-Oceans and Atmospheres 87, 2045-2056.

Bayon, G., German, C.R., Burton, K.W., Nesbitt, R.W., Rogers, N., 2004. Sedimentary Fe-Mn oxyhydroxides as paleoceanographic archives and the role of aeolian flux in regulating oceanic dissolved REE. Earth Planet. Sci. Lett. 224, 477-492.

Bayon, G., Vigier, N., Burton, K.W., Brenot, A., Carignan, J., Etoubleau, J., Chu, N.C., 2006. The control of weathering processes on riverine and seawater hafnium isotope ratios. Geology 34, 433-436.

Budillon, G., Salusti, E. and Tucci, S. 2006. The evolution of density currents and nepheloid bottom layers in the Ross Sea (Antarctica). Journal of Marine Research 64, 517–540.

Budillon, G., Castagno, P., Aliani, S., Spezie, G., Padman, L., 2011. Thermohaline variability and Antarctic bottom water formation at the Ross Sea shelf break. Deep-Sea Research Part I-Oceanographic Research Papers 58, 1002-1018.

Bouvier, A., Vervoort, J.D., Patchett, P.J., 2008. The Lu–Hf and Sm–Nd isotopic composition of CHUR: Constraints from unequilibrated chondrites and implications for the bulk composition of terrestrial planets. Earth Planet. Sci. Lett. 273, 48-57.

Capello, M., Budillon, G., Cutroneo, L. and Tucci, S., 2009. The nepheloid bottom layer and water masses at the shelf break of the western Ross Sea. Deep-Sea Research II 56, 843–858.

Carter, P., Vance, D., Hillenbrand, C.D., Smith, J.A., Shoosmith, D.R., 2012. The neodymium isotopic composition of waters masses in the eastern Pacific sector of the Southern Ocean. Geochim. Cosmochim. Acta 79, 41-59.

Chen, T.-Y., Frank, M., Haley, B.A., Gutjahr, M., Spielhagen, R.F., 2012. Variations of North Atlantic inflow to the central Arctic Ocean over the last 14 million years inferred from hafnium and neodymium isotopes. Earth Planet. Sci. Lett. 353, 82-92.

Chen, T.Y., Li, G.J., Frank, M., Ling, H.F., 2013a. Hafnium isotope fractionation during continental weathering: Implications for the generation of the seawater Nd-Hf isotope relationships. Geophys. Res. Lett. 40, 916-920.

Chen, T.Y., Stumpf, R., Frank, M., Beldowski, J., Staubwasser, M., 2013b. Contrasting geochemical cycling of hafnium and neodymium in the central Baltic Sea. Geochim. Cosmochim. Acta 123, 166-180.

David, K., Frank, M., O'Nions, R.K., Belshaw, N.S., Arden, J.W., 2001. The Hf isotope composition of global seawater and the evolution of Hf isotopes in the deep Pacific Ocean from Fe-Mn crusts. Chem. Geol. 178, 23-42.

Elderfield, H., Sholkovitz, E.R., 1987. Rare-earth elements in the pore waters of reducing nearshore sediments. Earth Planet. Sci. Lett. 82, 280-288.

Firdaus, M.L., Minami, T., Norisuye, K., Sohrin, Y., 2011. Strong elemental fractionation of Zr-Hf and Nb-Ta across the Pacific Ocean. Nature Geoscience 4, 227-230.

Firdaus, M.L., Norisuye, K., Nakagawa, Y., Nakatsuka, S., Sohrin, Y., 2008. Dissolved and labile particulate Zr, Hf, Nb, Ta, Mo and W in the western North Pacific Ocean. Journal of Oceanography 64, 247-257.

Frank, M., 2002. Radiogenic isotopes: Tracers of past ocean circulation and erosional input. Rev. Geophys. 40, 1001, doi:1010.1029/2000RG000094.

Godfrey, L.V., Field, M.P., Sherrell, R.M., 2008. Estuarine distributions of Zr, Hf, and Ag in the Hudson River and the implications for their continental and anthropogenic sources to seawater. Geochem. Geophys. Geosyst. 9, Q12007, doi: 12010.11029/12008GC002123.

Godfrey, L.V., White, W.M., Salters, V.J.M., 1996. Dissolved zirconium and hafnium distributions across a shelf break in the northeastern Atlantic Ocean. Geochim. Cosmochim. Acta 60, 3995-4006.

Godfrey, L.V., Zimmermann, B., Lee, D.C., King, R.L., Vervoort, J.D., Sherrell, R.M., Halliday, A.N., 2009. Hafnium and neodymium isotope variations in NE Atlantic seawater. Geochem. Geophys. Geosyst. 10, Q08015, doi: 08010.01029/02009gc002508.

Goldstein, S.L., Hemming, S.R., 2003. Long-lived isotopic tracers in oceanography, paleoceanography, and ice-sheet dynamics, in: Elderfield, H. (Ed.), Treatise on Geochemistry. Elsevier, Oxford, pp. 453–489.

Gutjahr, M., Frank, M., Stirling, C.H., Keigwin, L.D., Halliday, A.N., 2008. Tracing the Nd isotope evolution of North Atlantic deep and intermediate waters in the Western North Atlantic since the Last Glacial Maximum from Blake Ridge sediments. Earth Planet. Sci. Lett. 266, 61-77.

Haley, B.A., Klinkhammer, G.P., McManus, J., 2004. Rare earth elements in pore waters of marine sediments. Geochim. Cosmochim. Acta 68, 1265-1279.

Jacobs, S.S., Amos, A.F., Bruchhausen, P.M., 1970. Ross Sea oceanography and Antarctic Bottom Water formation. Deep-Sea Research 17, 935-962.

Jacobsen, S.B., Wasserburg, G.J., 1980. Sm-Nd Isotopic Evolution of Chondrites. Earth Planet. Sci. Lett. 50, 139-155.

Jeandel, C., Bishop, J.K., Zindler, A., 1995. Exchange of Neodymium and Its Isotopes between Seawater and Small and Large Particles in the Sargasso Sea. Geochim. Cosmochim. Acta 59, 535-547.

Kipf, A., Hauff. F., Werner, R., Gohl, K., van den Bogaard, P., Hoernle, K., Maichera, D., Klügel A. (in press). Seamounts off the West Antarctic Margin: a case fot non-hotspot driven intraplate volcanism. Gondwana Research.

Lacan, F., Jeandel, C., 2001. Tracing Papua New Guinea imprint on the central Equatorial Pacific Ocean using neodymium isotopic compositions and Rare Earth Element patterns. Earth Planet. Sci. Lett. 186, 497-512.

Lacan, F., Jeandel, C., 2005a. Acquisition of the neodymium isotopic composition of the North Atlantic Deep Water. Geochem. Geophys. Geosyst. 6.

Lacan, F., Jeandel, C., 2005b. Neodymium isotopes as a new tool for quantifying exchange fluxes at the continent-ocean interface. Earth Planet. Sci. Lett. 232, 245-257.

Little, S.H., Vance, D., Siddall, M., Gasson, E., 2013. A modeling assessment of the role of reversible scavenging in controlling oceanic dissolved Cu and Zn distributions. Glob. Biogeochem. Cyc. 27, doi: 10.1002/gbc.20073.

McKelvey, B.A., Orians, K.J., 1993. Dissolved zirconium in the North Pacific Ocean. Geochim. Cosmochim. Acta 57, 3801-3805.

McKelvey, B.A., 1994. The marine geochemistry of Zr and Hf, PhD Thesis, Univ. British Columbia.

McKelvey, B.A., Orians, K.J., 1998. The determination of dissolved zirconium and hafnium from seawater using isotope dilution inductively coupled plasma mass spectrometry. Mar. Chem. 60, 245-255.

Mukasa, S.B., Dalziel, I.W.D., 2000. Marie Byrd Land, West Antarctica: Evolution of Gondwana's Pacific margin constrained by zircon U-Pb geochronology and feldspar common-Pb isotopic compositions. Geological Society of America Bulletin 112 611-627.

Nowell, G.M., Kempton, P.D., Noble, S.R., Fitton, J.G., Saunders, A.D., Mahoney, J.J., Taylor, R.N., 1998. High precision Hf isotope measurements of MORB and OIB by thermal ionisation mass spectrometry: insights into the depleted mantle. Chem. Geol. 149, 211-233.

Orsi, A.H., Johnson, G.C., Bullister, J.L., 1999. Circulation, mixing, and production of Antarctic Bottom Water. Prog. Oceanogr. 43, 55-109.

Orsi, A., Whitworth, T., 2005. Hydrographic Atlas of the World Ocean Circulation Experiment (WOCE). Volume 1: Southern Ocean. In: Sparrow, M.,

Chapman, P., Gould, J. (Eds.). International WOCE Project Office,Southampton, UK ISBN 0-904175-49-9.

Orsi, A.H., Whitworth, T., Nowlin, W.D., 1995. On the meriodional extent and fronts of the Antarctic Circumpolar Current. Deep-Sea Research Part I-Oceanographic Research Papers 42, 641-673.

Orsi, A.H., Wiederwohl, C.L., 2009. A recount of Ross Sea waters. Deep-Sea Research Part II-Topical Studies in Oceanography 56, 778-795.

Pankhurst, R.J., Weaver, S.D., Bradshaw, J.D., Storey, B.C., Ireland, T.R., 1998. Geochronology and geochemistry of pre-Jurassic superterranes in Marie Byrd Land, Antarctica. Journal of Geophysical Research 103, 2529-2547.

Pearce, C.R., Jones, M.T., Oelkers, E.H., Pradoux, C., Jeandel, C., 2013. The effect of particulate dissolution on the neodymium (Nd) isotope and Rare Earth Element (REE) composition of seawater. Earth Planet. Sci. Lett. 369–370, 138-147.

Piotrowski, A.M., Goldstein, S.L., Hemming, S.R., Fairbanks, R.G., 2005. Temporal relationships of carbon cycling and ocean circulation at glacial boundaries. Science 307, 1933-1938.

Piotrowski, A.M., Lee, D.C., Christensen, J.N., Burton, K.W., Halliday, A.N., Hein, J.R., Günther, D., 2000. Changes in erosion and ocean circulation recorded in the Hf isotopic compositions of North Atlantic and Indian Ocean ferromanganese crusts. Earth Planet. Sci. Lett. 181, 315-325.

Rempfer, J., Stocker, T.F., Joos, F., Dutay, J.-C., Siddall, M., 2011. Modelling Nd-isotopes with a coarse resolution ocean circulation model: Sensitivities to model parameters and source/sink distributions. Geochim. Cosmochim. Acta 75, 5927-5950.

Rickli, J., Frank, M., Baker, A.R., Aciego, S., de Souza, G., Georg, R.B., Halliday, A.N., 2010. Hafnium and neodymium isotopes in surface waters of the eastern Atlantic Ocean: Implications for sources and inputs of trace metals to the ocean. Geochim. Cosmochim. Acta 74, 540-557.

Rickli, J., Frank, M., Halliday, A.N., 2009. The hafnium-neodymium isotopic composition of Atlantic seawater. Earth Planet. Sci. Lett. 280, 118-127.

Rickli, J., Frank, M., Stichel, T., Georg, R.B., Vance, D., Halliday, A.N., 2013. Controls on the incongruent release of hafnium during weathering of metamorphic and sedimentary catchments. Geochim. Cosmochim. Acta 101, 263-284.

Rudnick, R.L., Gao, S., 2003. Composition of the Continetal Crust, in: Rudnick, R.L. (Ed.), Treatise on Geochemistry. Elsevier, Oxford, pp. 1-64.

Rutberg, R.L., Hemming, S.R., Goldstein, S.L., 2000. Reduced North Atlantic Deep Water flux to the glacial Southern Ocean inferred from neodymium isotope ratios. Nature 405, 935-938.

Siddall, M., Khatiwala, S., van de Flierdt, T., Jones, K., Goldstein, S.L., Hemming, S., Anderson, R.F., 2008. Towards explaining the Nd paradox using reversible scavenging in an ocean general circulation model. Earth Planet. Sci. Lett. 274, 448-461.

Stichel, T., Frank, M., Rickli, J., Haley, B.A., 2012a. The hafnium and neodymium isotope composition of seawater in the Atlantic sector of the Southern Ocean. Earth Planet. Sci. Lett. 317, 282-294.

Stichel, T., Frank, M., Rickli, J., Hathorne, E.C., Haley, B.A., Jeandel, C., Pradoux, C., 2012b. Sources and input mechanisms of hafnium and neodymium in surface

waters of the Atlantic sector of the Southern Ocean. Geochim. Cosmochim. Acta 94, 22-37.

Talley L., Pickard G., Emery W., J., S., 2011. Chapter 13: Southern Ocean, Descriptive Physical Oceanography. Elsevier Ltd.

Tazoe, H., Obata, H., Gamo, T., 2006. Vertical profiles of cerium and neodymium isotopic compositions and REEs pattern in the Ross Sea. Geochim. Cosmochim. Acta 70, A640.

van de Flierdt, T., Hemming, S.R., Goldstein, S.L., Abouchami, W., 2006. Radiogenic isotope fingerprint of Wilkes Land - Adelie Coast Bottom Water in the circum-Antarctic Ocean. Geophys. Res. Lett. 33, L12606, doi: 12610.11029/12006GL026020.

van de Flierdt, T., Frank, M., Halliday, A.N., Hein, J.R., Hattendorf, B., Gunther, D., Kubik, P.W., 2004. Deep and bottom water export from the Southern Ocean to the Pacific over the past 38 million years. Paleoceanography 19, art. no.-PA1020.

van de Flierdt, T., Frank, M., Lee, D.C., Halliday, A.N., 2002. Glacial weathering and the hafnium isotope composition of seawater. Earth Planet. Sci. Lett. 201, 639-647.

Vervoort, J.D., Blichert-Toft, J., 1999. Evolution of the depleted mantle: Hf isotope evidence from juvenile rocks through time. Geochim. Cosmochim. Acta 63, 533-556.

Vervoort, J.D., Plank, T., Prytulak, J., 2011. The Hf-Nd isotopic composition of marine sediments. Geochim. Cosmochim. Acta 75, 5903-5926.

Wadham, J.L., Tranter, M., Skidmore, M., Hodson, A.J., Priscu, J., Lyons, W.B., Sharp, M., Wynn, P., Jackson, M., 2010. Biogeochemical weathering under ice: Size matters. Glob. Biogeochem. Cyc. 24.

Whitworth, T., Orsi, A.H., Kim, S.-J., Nowlin, W.D., 1998. Water masses and mixing near the Antarctic Slope Front. Ocean, Ice and Atmosphere: Interactions at the Antarctic Continental Margin, 1-27.

Wilson, D.J., Piotrowski, A.M., Galy, A., McCave, I.N., 2012. A boundary exchange influence on deglacial neodymium isotope records from the deep western Indian Ocean. Earth Planet. Sci. Lett. 341, 35-47.

Zimmermann, B., Porcelli, D., Frank, M., Andersson, P.S., Baskaran, M., Lee, D.C., Halliday, A.N., 2009a. Hafnium isotopes in Arctic Ocean water. Geochim. Cosmochim. Acta, 3218-3233.

Zimmermann, B., Porcelli, D., Frank, M., Rickli, J., Lee, D.-C., Halliday, A.N., 2009b. The hafnium isotope composition of Pacific Ocean water. Geochim. Cosmochim. Acta 73, 91-101.

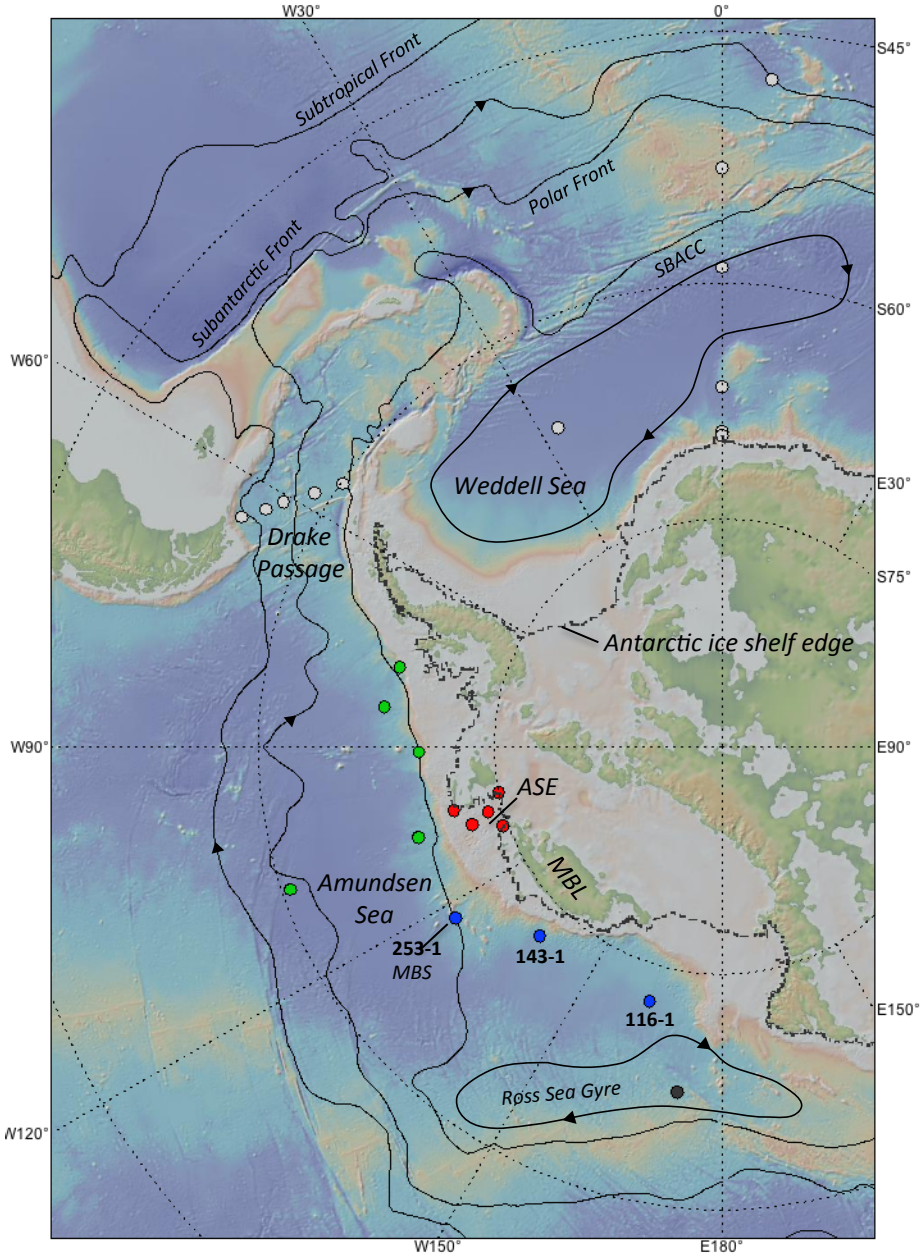
W30°
0°
S45°
Subtropical Front
Polar Front
Subantarctic Front
SBACC
S60°
W60°
Weddell Sea
E30°
Drake
Passage
S75°
Antarctic ice shelf edge
W90°
E90°
ASE
MBL
Amundsen
Sea
253-1
MBS
143-1
116-1
E150°
Ross Sea Gyre
W120°
W150°
E180°

Figure 1.

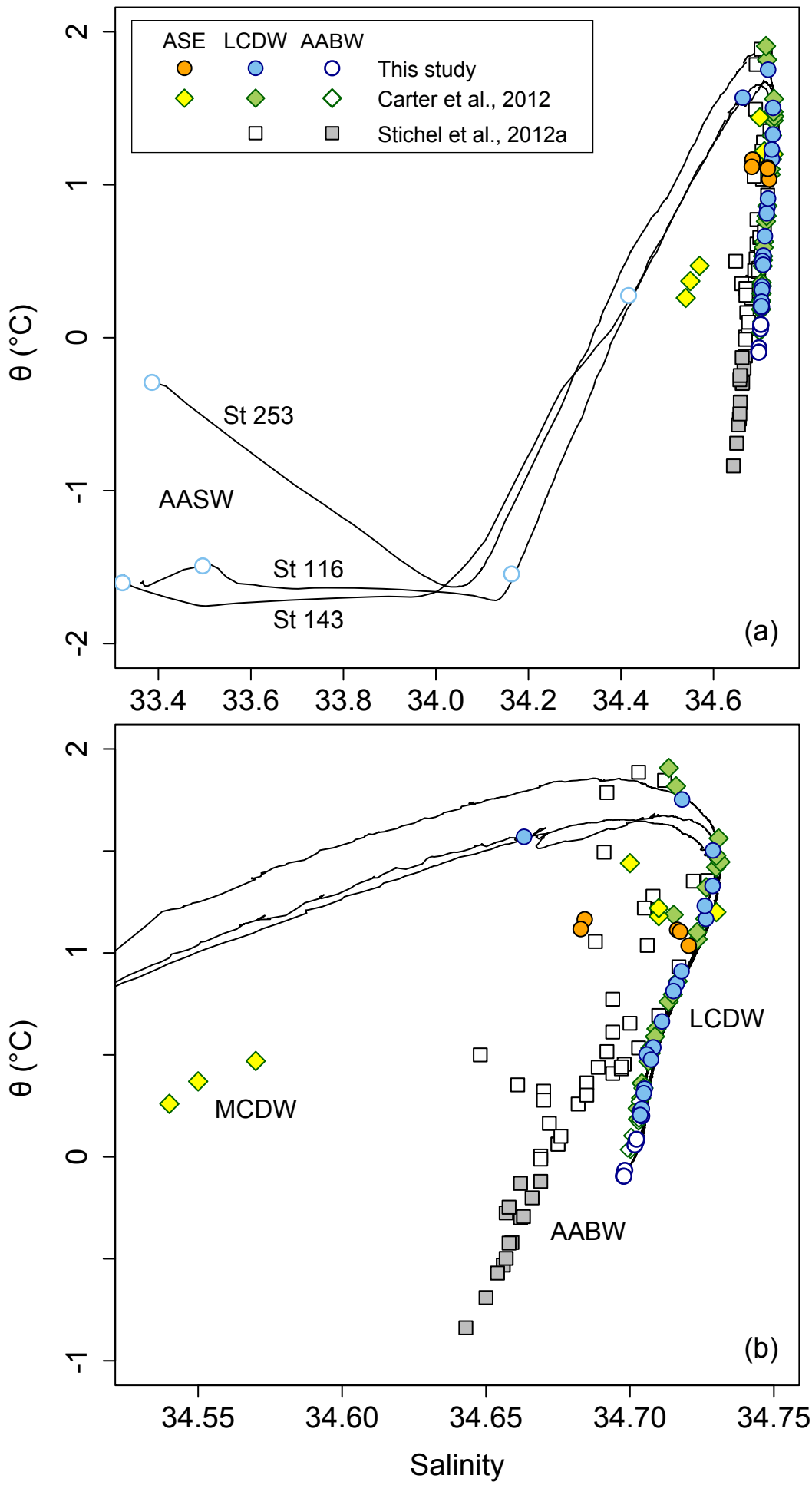
ASE
LCDW
AABW
This study
Carter et al., 2012
Stichel et al., 2012a
St 253
AASW
St 116
St 143
(a)
θ (°C)
2
1
0
-1
-2
33.4
33.6
33.8
34.0
34.2
34.4
34.6
LCDW
MCDW
AABW
(b)
34.55
34.60
34.65
34.70
34.75
Salinity

Fig 2

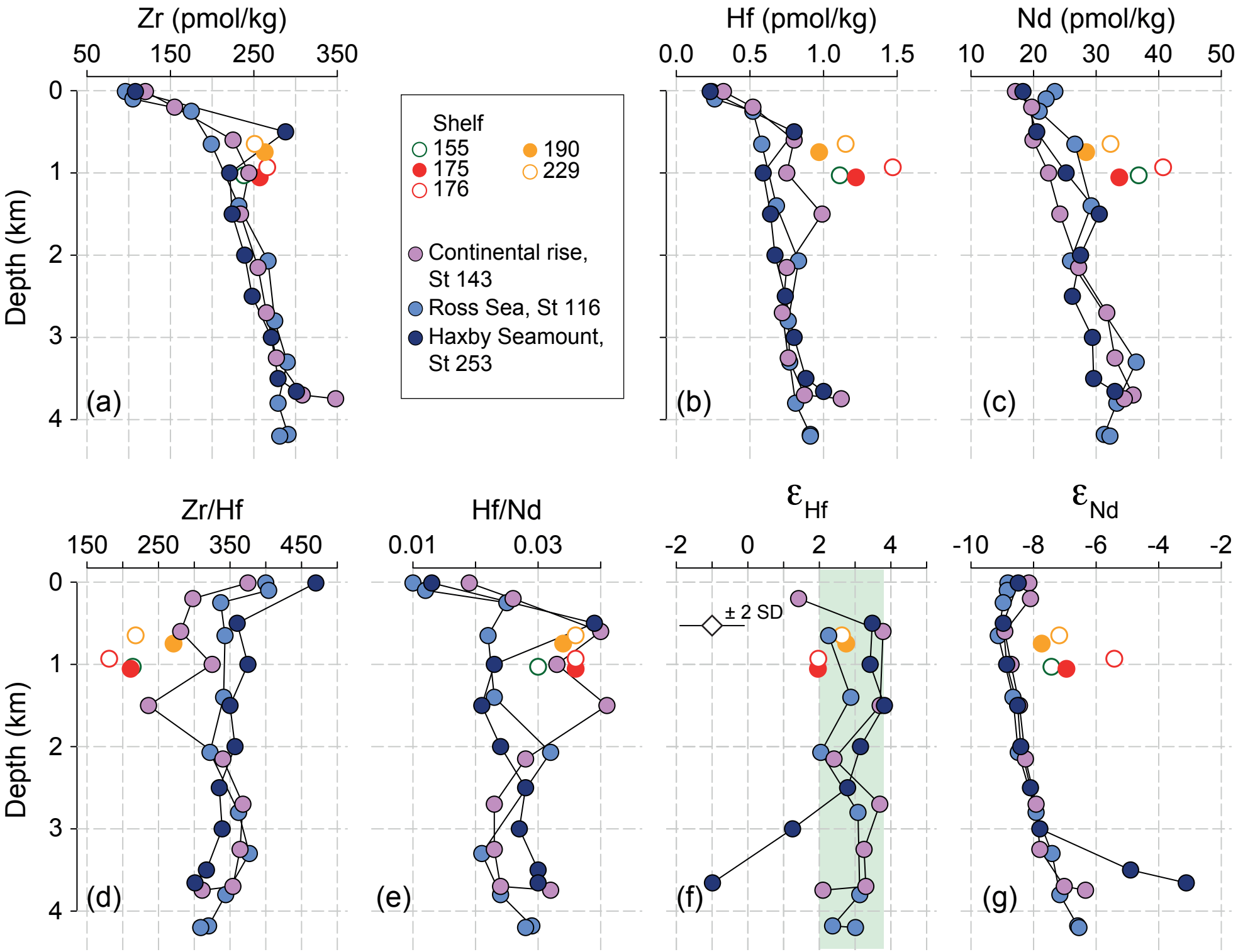
Zr (pmol/kg)
50
150
250
350
Hf (pmol/kg)
0.0
0.5
1.0
1.5
Nd (pmol/kg)
10
20
30
40
50
Depth (km)
0
1
2
3
4
(a)
(b)
(c)
Shelf
155
175
176
190
229
Continental rise, St 143
Ross Sea, St 116
Haxby Seamount, St 253
Zr/Hf
150
250
350
450
Hf/Nd
0.01
0.03
ε_{Hf}
-2
0
2
4
± 2 SD
ε_{Nd}
-10
-8
-6
-4
-2
(d)
(e)
(f)
(g)

Fig 3

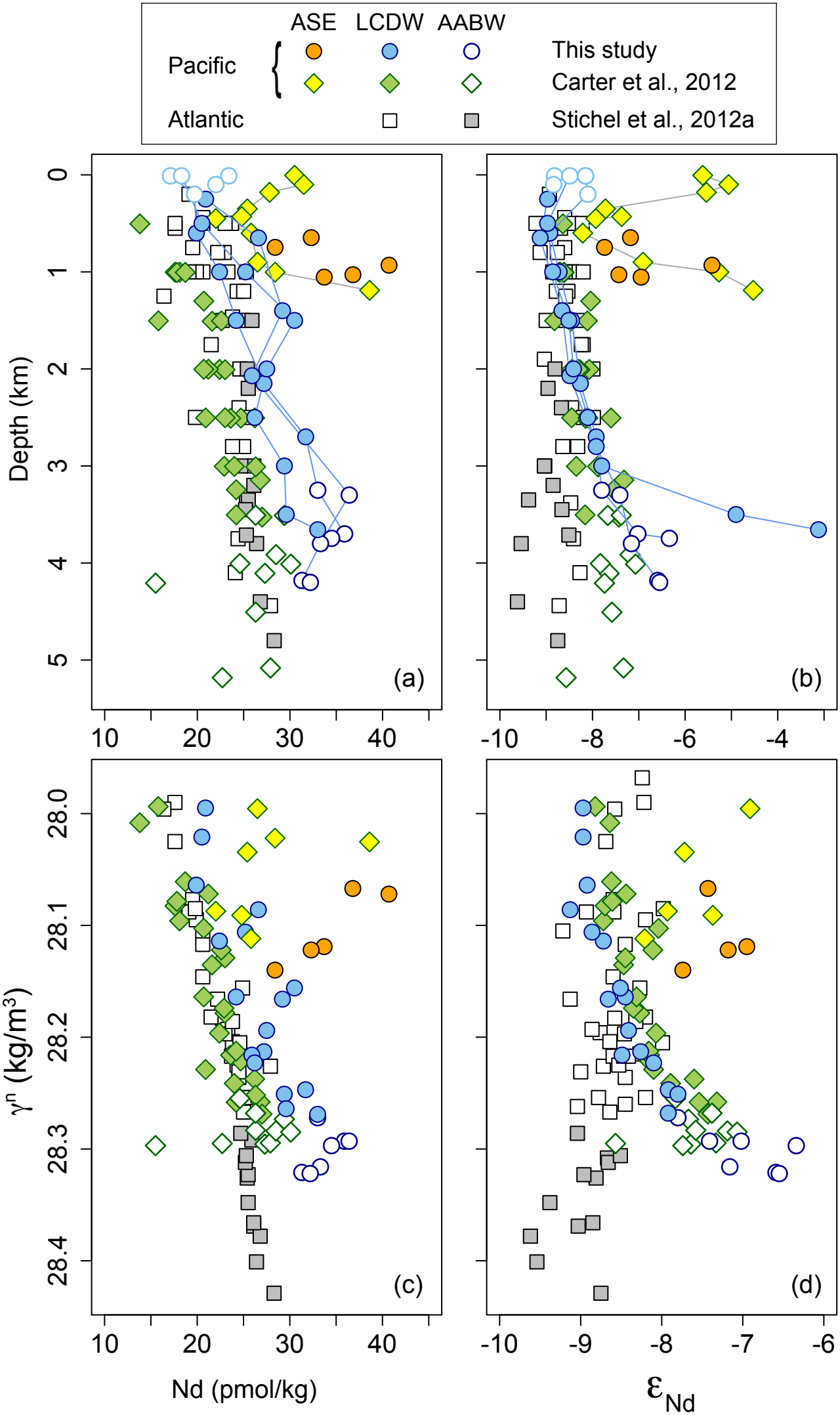
ASE
LCDW
AABW
Pacific
Atlantic
This study
Carter et al., 2012
Stichel et al., 2012a
Depth (km)
(a)
(b)
(c)
(d)
γn (kg/m3)
Nd (pmol/kg)
εNd

Fig 4

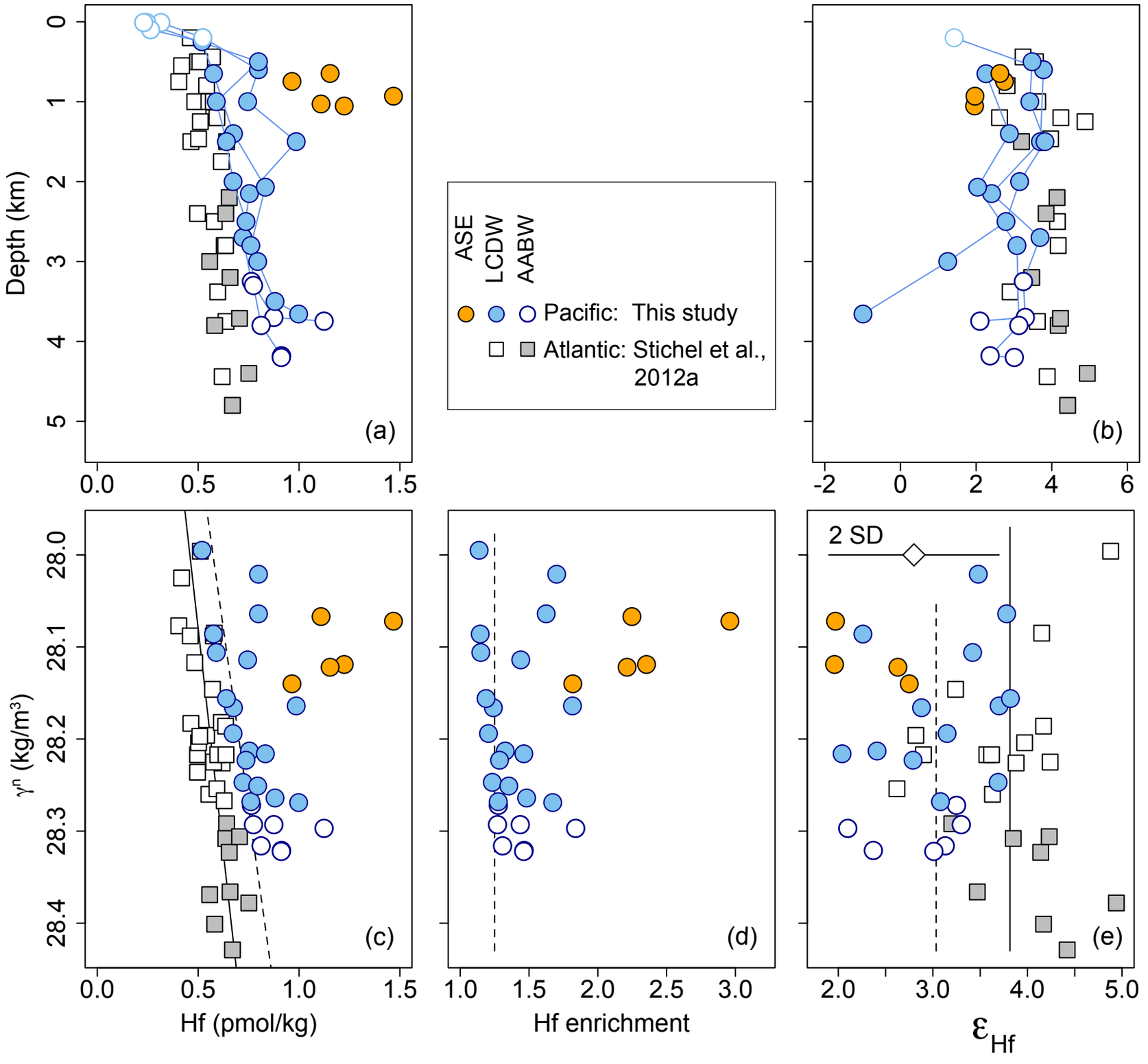
Depth (km)
0
1
2
3
4
5
0.0
0.5
1.0
1.5
(a)
ASE
LCDW
AABW
Pacific: This study
Atlantic: Stichel et al., 2012a
-2
0
2
4
6
(b)
γ^n (kg/m^3)
28.0
28.1
28.2
28.3
28.4
(c)
Hf (pmol/kg)
(d)
Hf enrichment
2 SD
(e)
2.0
3.0
4.0
5.0
ε_{Hf}

Fig. 5

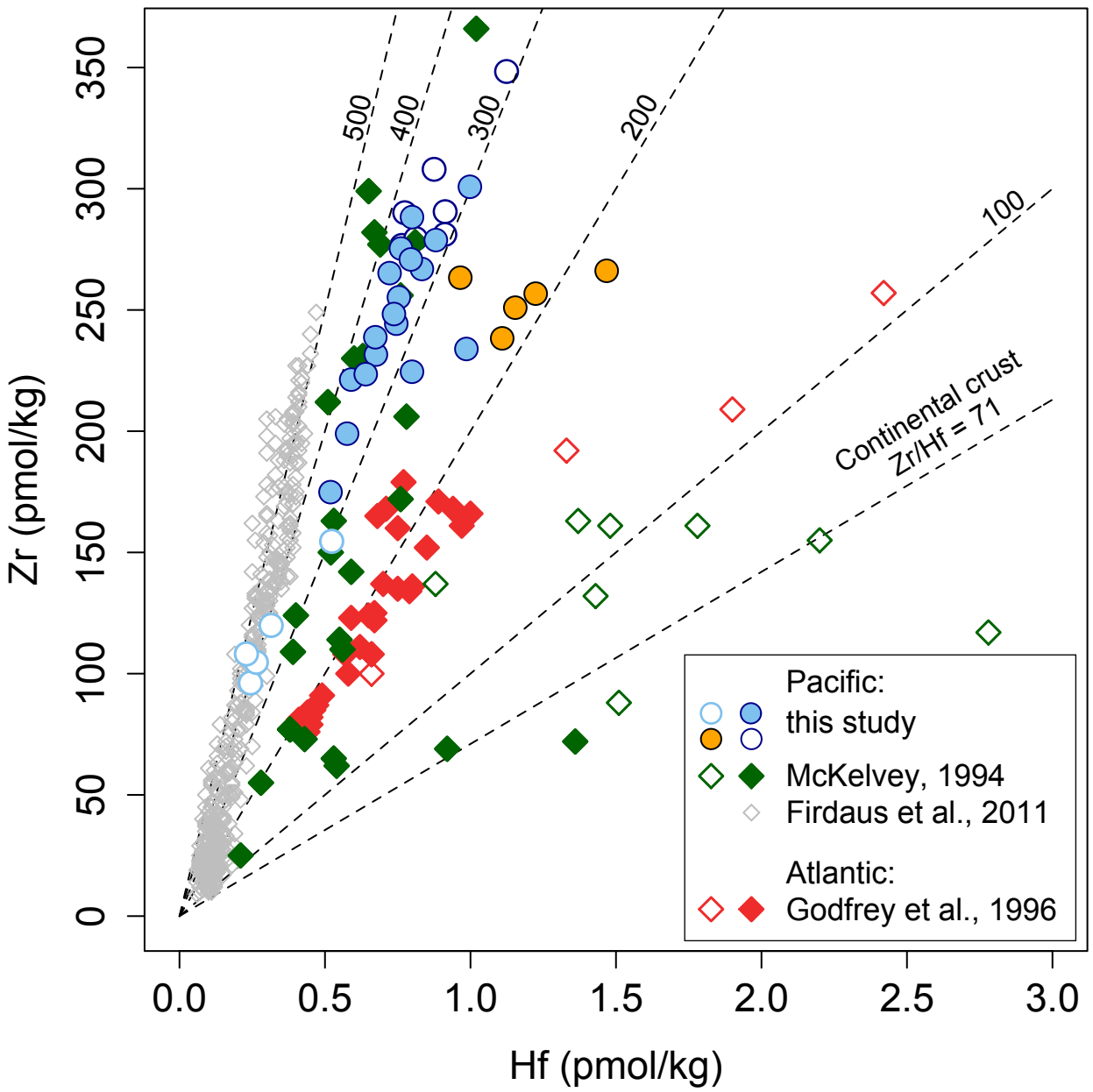
Zr (pmol/kg)
Hf (pmol/kg)
0
50
100
150
200
250
300
350
0.0
0.5
1.0
1.5
2.0
2.5
3.0
500
400
300
200
100
Continental crust
Zr/Hf = 71
Pacific:
this study
McKelvey, 1994
Firdaus et al., 2011
Atlantic:
Godfrey et al., 1996

Fig. 6

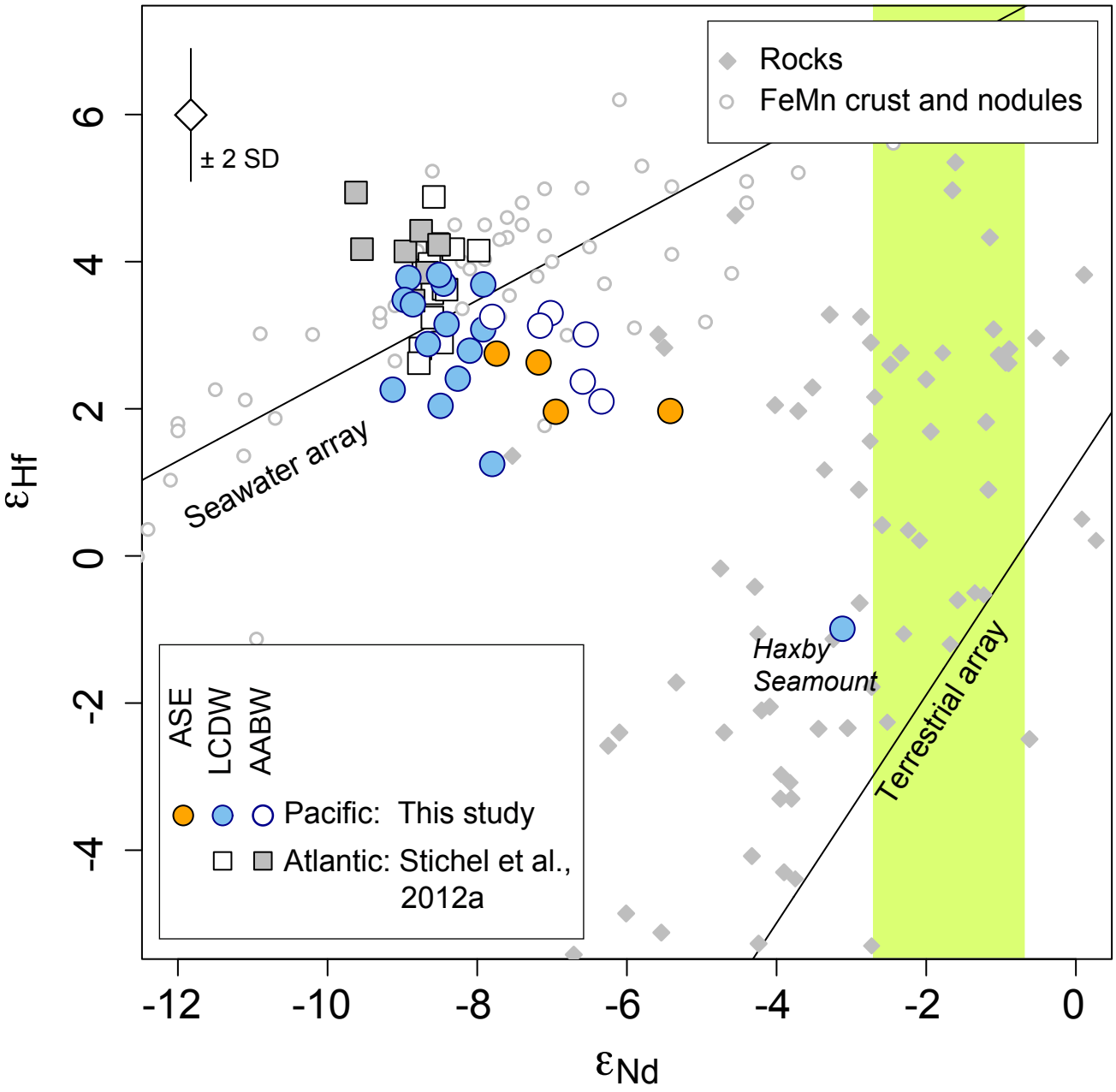
Rocks
FeMn crust and nodules
± 2 SD
Seawater array
Terrestrial array
Haxby Seamount
ASE
LCDW
AABW
Pacific: This study
Atlantic: Stichel et al., 2012a
εHf
εNd
6
4
2
0
-2
-4
-12
-10
-8
-6
-4
-2
0

Fig 7